

# NUMERICAL SIMULATION OF DAMAGE AND FAILURE OF COMPOSITE PRESSURE VESSELS

## Jörg Bernhard Multhoff

Department for Mathematical Models in Materials Science (MMW)  
Aachen University of Technology (RWTH Aachen)  
Augustinerbach 4-22, 52064 Aachen, Germany  
multhoff@mmw.rwth-aachen.de

## Luís Eduardo Vergueiro Loures da Costa

Centro Técnico Aeroespacial (CTA/IAE/ASE)  
Praça Mal.-do-Ar Eduardo Gomes, 50  
São José dos Campos (SP), CEP 12228-904, Brazil  
loures@iae.cta.br

## Jens Krieger

Department for Mathematical Models in Materials Science (MMW)  
Aachen University of Technology (RWTH Aachen)  
krieger@mmw.rwth-aachen.de

## Josef Betten

Department for Mathematical Models in Materials Science (MMW)  
Aachen University of Technology (RWTH Aachen)  
betten@mmw.rwth-aachen.de

**Abstract.** *In comparison to conventional metallic materials, where the theory of plasticity is well established and corresponding algorithms are standard procedures in all commercial finite element codes, the inelastic analysis of composite materials is currently a developing field. A proper failure analysis of composite structures is still to be established. This work discusses the implementation of failure criteria and property degradation models in a finite element program to simulate damage and failure of composite structures. These procedures are applied to the analysis of the S33 composite pressure vessel used as solid rocket motor case in the Brazilian space program. The computational results are confronted with experimental data gathered in hydrostatic burst tests. The resulting discussion highlights the significance of inelastic computations for optimized composite structures as well as capabilities and shortcomings of the different failure and property degradation theories. One result of particular interest is the insight gained in the robust behavior of composite structures - they can achieve high failure loads despite extensive prior damage.*

**Keywords.** *Composite Pressure Vessel, Finite Element Analysis, Damage Mechanics, Failure Criteria.*

## 1. Introduction

Solid rocket motor cases act mainly as pressure vessels and are frequently made from fiber reinforced composites by filament winding. In this way the full potential of composite materials can be exploited. Furthermore the manufacturing process is cost effective. The technology of rocket propulsion including solid rockets is described by Sutton (1992) and filament winding is presented in the classic work of Rosato and Grove (1964). Policelli et al (1987) treat the application of composites for space and missile structures like motor cases.

Design and analysis of composite structures is considerably more complex than the design of structures made from more traditional engineering materials like steel or aluminum. This is because composite structures are usually layered and have anisotropic characteristics, which means that much more information must be specified and analyzed. Furthermore the mechanics of composite structures is complicated by the possible coupling between extensional, bending and shearing deformation modes and the greater variety of failure modes (Jones, 1999). Effective and efficient computational tools are necessary to help in the design of optimized composite structures.

The Institute for Aeronautics and Space (IAE) develops solid rocket motors as the propulsion of sounding rockets and satellite launchers. Major projects are the VLS and VLM launch vehicles described e. g. in Isakowitz et al (1999). The solid rocket motor cases for the upper stages of these vehicles are manufactured from composite materials by filament winding to achieve minimum weight and maximum payload. These composite cases are currently analyzed in cooperation with the Department for Mathematical Models in Material Science (MMW) of the Aachen University of Technology (RWTH). The focus of this investigation are the failure modes under internal pressure and the prediction of the burst pressure. These are decisive factors in the design of light-weight pressure vessels. A proper understanding of these factors leads to optimized designs for future composite rocket motor cases and pressure vessels. Both experimental and computational methods are used in the investigation. Loures et al (2001) discuss the structural development of composite motor cases including their experimental qualification. Krieger et al (2001) present a three-dimensional high-resolution finite element model for a composite motor case under internal pressure and compare the analysis results with experimental

data. Some of the problems encountered in the development of these high-resolution finite element models are described in Multhoff et al (2001).

The purpose of the present work is the implementation of failure/post-failure models for fiber-reinforced composite materials into an overall progressive degradation procedure for the burst pressure prediction of composite pressure vessels. The resulting procedure is applied to the S33 rocket motor case.

## 2. Finite Element Modeling of Composite Rocket Motor Cases

The finite element analysis of composite laminates is treated in the textbook of Ochoa and Reddy (1992). Specific issues of finite elements applied to composite materials are outlined in a review article by Wood (1994). Several examples for finite element analyses of composite rocket motor cases or composite pressure vessels can be found in the literature. The following authors discuss the bursting problem under internal pressure:

- Gramoll et al (1990): Axisymmetric quadratic volume elements are used for the analysis of a solid rocket motor case. Three elements in thickness direction are used, but it is not clear how the lay-up was represented in the model.
- Doh and Hong (1995): Three-dimensional quadratic layered shell elements are specifically developed to treat the bursting problem of a composite motor case. A 90° sector model is analyzed using symmetry displacement boundary conditions.
- Ore (1998): Axisymmetric volume elements are used to simulate the failure of a composite over-wrapped spherical metal pressure vessel. An unstructured mesh is used and individual layers of the composite material are not represented. Equivalent orthotropic material properties are used instead.
- Pereira and Palmerio (1998): Three-dimensional quadratic layered shell elements are used for the analysis of a composite case. A 90° sector model with symmetry displacement boundary conditions is considered.
- Sun et al (1999): Axisymmetric volume elements are specifically developed for the analysis of a composite rocket motor case. The number of elements in thickness direction and the representation of the lay-up are not discussed.

This account makes no claim of completeness, but it can be seen that mostly either axisymmetric elements or layered shell elements were used in the past. All references consider an axisymmetric structure and state that a geometrically nonlinear analysis is necessary because of the relatively large displacements encountered for thin walled pressure vessels.

An alternative to the approaches discussed so far is the use of three-dimensional volume elements. Elements with orthotropic properties could be used to resolve individual layers or to represent multiple layers using equivalent properties. This would lead either to an excessive number of elements or to a cumbersome pre- and post-processing. A good compromise is the use of layered volume elements. Three-dimensional volume elements offer the greatest modeling flexibility but lead obviously to the highest computational effort. This fact prevented their use for the full-scale analysis of composite pressure vessels in the past.

The element used in this study is the Solid 46 element available in the ANSYS program. This layered volume element is a linear eight node hexaeder with additional incompatible quadratic shape functions to improve the bending behavior. For the through-thickness integration a formulation similar to the one used for layered shell elements is employed. This element type was selected because the objective of this study is the detailed simulation of failure modes and the accurate prediction of the burst pressure. Therefore regions of geometric complexity must be represented adequately.

## 3. Parameterized Finite Element Models

An important feature of the analysis concept underlying the present study is that the finite element model is flexibly generated by an automated preprocessor on the basis of user-specified parameters. The parameters are defined by the geometry of the pressure vessel to be analyzed and the mesh density of the desired finite element model. The last aspect is essential because it allows the user to scale the computational effort with respect to the required accuracy. The models for the present study are created in three basic steps: In the first step, contour, winding angle and thickness distributions of the pressure vessel are calculated on the basis of netting analysis equations for either planar or geodetic winding and using theoretical or empirical models for the wall thickness distribution. These calculations depend on user-specified parameters like diameter, length and filament band width. The results of this step are collected in data tables. In the second step, a Solid Geometry model of the pressure vessel is created on the basis of the data tables from the first step and additional parameters selected by the user. In the third step, the finite element model consisting of structured meshes is created by mapped meshing. Structured meshes are most appropriate for the selected layered volume elements. Mesh densities can be controlled by the user through the selection of further parameters. Figure (1) shows a solid geometry model (left) and the associated finite element model (right) for the S33 rocket motor case. In this case, a 20° sector model with four elements in circumferential and one element in thickness direction was created by the preprocessor.

As already pointed out, filament wound shells for rocket motor cases or pressure vessels are usually considered to be axisymmetric solids. This is not entirely correct because the filament placement in the winding process is not strictly axisymmetric, which leads to non-axisymmetric lay-up and section thickness. The magnitude of deviation from an axisymmetric configuration depends on the selected winding pattern. This deviation is usually neglected because it is perceived to be small, complicated to measure and difficult to model. The present work follows this line of thinking.

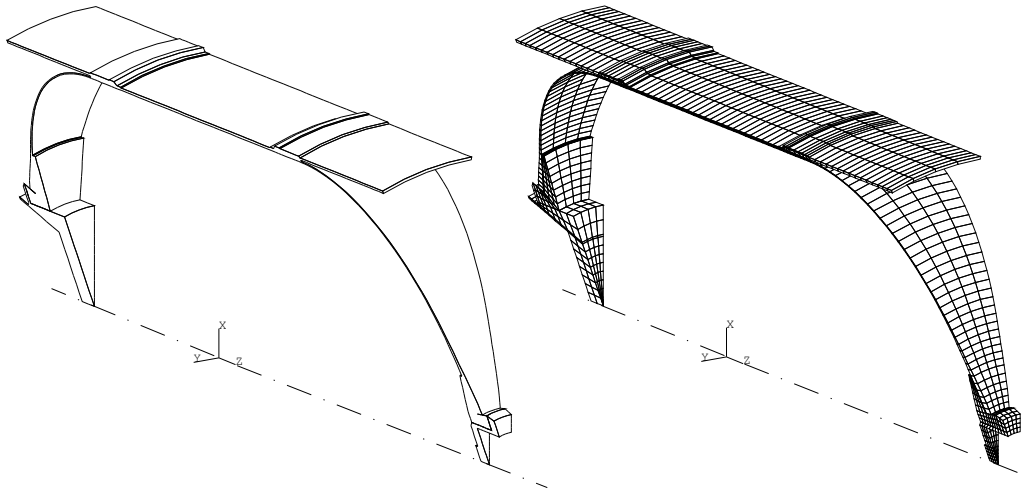


Figure 1. Solid geometry model and finite element mesh (20° sector) for the S33 rocket motor case.

For the bursting problem under internal pressure both domain and data of the underlying mathematical problem are accepted to be axisymmetric. Hence an axisymmetric solution is expected. Namely the displacement vector field in cylindrical coordinates  $\vec{u}(r, \theta, z)$  is independent of the circumferential coordinate  $\theta$ . However, this does *not* necessarily mean that the circumferential component of the displacement vector  $u_\theta = \vec{e}_\theta \cdot \vec{u}$  is zero. This is because un-symmetric laminates can exhibit extension-shear coupling (Jones, 1999). An axisymmetric filament wound composite shell will generally twist under internal pressure. The vessel under consideration shows this behavior. For the same reason, sections in the meridian plane will warp in general. The standard formulation for axisymmetric volume elements can not represent this effect. Furthermore, this formulation requires the  $\theta$ -direction to be a principal material direction.

When three-dimensional shell or volume elements are used to model axisymmetric structures under axisymmetric loading it is clearly not appropriate to construct full 360° meshes. The effort for the discretization in the circumferential direction would be both tremendous and senseless. If a reduced sector model is used, the problem of boundary conditions for the sections in the meridian plane arises. In the literature, 90° sector models with *so-called* axisymmetric boundary conditions are frequently encountered, Fig. (2) on the left (Doh et al, 1995; Pereira et al, 1998).

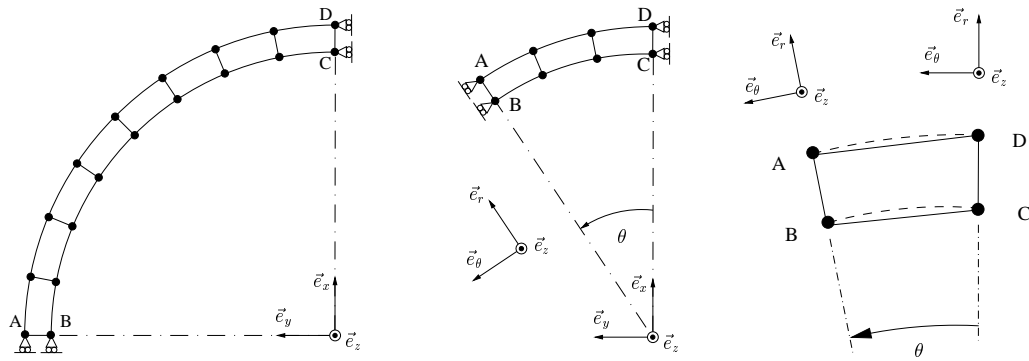


Figure 2. Symmetry Boundary Conditions and Axisymmetric Constraints.

In this study, the problem of boundary conditions for the sections in the meridian planes is evaded altogether. Coupling conditions in the global cylindrical coordinate system are used instead to enforce an axisymmetric solution (ANSYS command `CP`). For this purpose reference frames parallel to the local basis vectors of the cylindrical coordinates are defined at *all* nodes (ANSYS command `nrotat`). Accordingly the components of the displacement vector field with respect to these bases, namely  $(u_r, u_\theta, u_z)$ , will be the independent degrees of freedom (DOF). All stiffness and force components are transformed to cylindrical coordinates. This is a standard procedure handled by the finite element program system automatically. The following DOF coupling conditions would be used for the example on the right side in Fig. (2):

$$\begin{aligned} u_r|_A &= u_r|_D & u_\theta|_A &= u_\theta|_D & u_z|_A &= u_z|_D \\ u_r|_B &= u_r|_C & u_\theta|_B &= u_\theta|_C & u_z|_B &= u_z|_C \end{aligned}$$

In effect the displacement components at nodes *A* and *B* are no longer independent degrees of freedom. They are considered to be tied to the corresponding DOF at the 'master' nodes *C* and *D*. This can be achieved within finite element procedures by assigning identical equation numbers to sets of coupled DOF. In this case stiffness and force components of a coupled DOF will be assembled in the same matrix positions as the components of the associated 'master' DOF.

No boundary conditions on sections in a meridian plane are necessary if this procedure is used. An axisymmetric solution including displacements in circumferential direction will be found. This was verified with meshes containing multiple elements in the circumferential direction like the one shown in Fig. (1) as well as with full 360° meshes. By comparing the solution for nodes on different meridian planes it was also shown that no artificial stresses are induced. According to this result it is clear that only *one* element in circumferential direction is necessary for this kind of analysis. While the *numerical* solution is *strictly* independent of the number of elements in circumferential direction it is not independent of the circumferential angle  $\Delta\theta$  spanned by one element. This depends on the element formulation and is related to the aspect ratio of the element. For instance, the through-thickness integration scheme of the element type used for this study is reported to make increasing errors for increasing angles between those element faces, which are not parallel to the layers. The angle  $\Delta\theta$  should therefore be minimized under the constraint that the element aspect ratio is acceptable. It was verified, that under these conditions the solution converges under mesh refinement in the same way as the solution for a full 360° mesh.

#### 4. Failure Criteria and Degradation Models

A great number of different failure criteria and post-failure theories for composite materials have been proposed in the past (Nahas, 1986). For the purpose of this study only the models proposed by Tsai (Tsai, 1992; Liu and Tsai, 1998) and Chang (Chang et al 1987) are considered. The model proposed by Tsai was selected because it is based on the well-known Tsai-Wu failure criterion, which is implemented in most commercial finite element codes. This model was also used by Pereira et al (1998) to analyze the S44 composite rocket motor case. The model of Chang is based on the Hashin failure criteria and thus contains an explicit distinction of the most important failure modes of fiber-reinforced composites. This model was previously used by Doh and Hong (1995) for a study similar to the one of the present paper.

##### 4.1 Tsai Model

The failure and post-failure model of Tsai is based on the quadratic Tsai-Wu (1971) failure criterion, which can be represented as a scalar tensor polynomial involving the stress tensor  $S_i$ , a second-order strength tensor  $F_i$  and a forth-order strength tensor  $F_{ij}$  (These tensors are written in compressed notation here):

$$f = F_i S_i + F_{ij} S_i S_j \quad i, j = 1, 2, \dots, 6 \quad (1)$$

In the plane-stress case, the components of the strength tensors can be expressed through the basic uniaxial strength values as follows:

$$F_1 = \frac{1}{R_{11}^+} - \frac{1}{R_{11}^-}, \quad F_2 = \frac{1}{R_{22}^+} - \frac{1}{R_{22}^-}, \quad F_{11} = \frac{1}{R_{11}^+ R_{11}^-}, \quad F_{22} = \frac{1}{R_{22}^+ R_{22}^-}, \quad F_{66} = \frac{1}{(R_6)^2}$$

The interaction term  $F_{12}$  can be defined in several different ways:

- Based on biaxial tensile strength  $R_{biax}^+$

$$F_{12} = \frac{1}{2} \left( \frac{1 - R_{biax}^+ (F_1 + F_2)}{(R_{biax}^+)^2} - F_{11} - F_{22} \right)$$

- Based on 45° off-axis tensile strength  $R_{45}^+$

$$F_{12} = \frac{2}{R_{45}^+} - (F_1 + F_2) - \frac{1}{2}(F_{11} + F_{22} + F_{66})$$

- Arbitrary specification (with  $-1 < F_{12}^* < 1$ )

$$F_{12} = F_{12}^* \frac{1}{\sqrt{R_{11}^+ R_{11}^- R_{22}^+ R_{22}^-}}$$

- "Generalized Von Mises"

$$F_{12} = -\frac{1}{2} \frac{1}{\sqrt{R_{11}^+ R_{11}^- R_{22}^+ R_{22}^-}}$$

The definition of  $F_{12}$  is not unique and it's experimental determination is difficult. Liu et al (1998) use  $F_{12}^* = -1/2$  ("Generalized Von Mises"). Several other well-known failure criteria (Tsai-Hill, Hoffman) can be interpreted as degenerated/simplified cases of the Tsai-Wu criterion.

The Tsai Model assumes initiation of ply-failure once the tensor polynomial in Eqn. (1) reaches the value 1. Since the Tsai-Wu criterion can not directly differentiate between different failure modes, the following artifice is used: If the transverse in-plane strain component is positive, matrix cracking is assumed. Otherwise, matrix cracking is believed not to be possible and fiber breakage is assumed. Once matrix cracking or fiber breakage is identified, a selective degradation of material properties is proposed. In this way a ply can degrade twice only if the first failure is identified as matrix cracking. The second occurrence of failure will have to be fiber cracking. If the first failure is identified as fiber breakage only one degradation is possible. For further details Tsai (1992) and Liu and Tsai (1998) should be consulted.

#### 4.2 Chang Model

Chang et al (1987) proposed an extended version of Hashin's (1980) failure criteria to include the effect of non-linear shear-stress/shear-strain characteristics of many polymeric fiber reinforced composites. The criteria were further extended to contain a sub-mode for fiber-matrix shearing failure. For this study the linear version of Chang's criteria using the following sub-criteria are used:

- Fiber – Tension ( $S_1 > 0$ )

$$f_f^+ = \left( \frac{S_1}{R_{11}^+} \right)^2 + \left( \frac{S_6}{R_6} \right)^2 \quad (2)$$

– fiber breakage dominated sub-case

$$\left( \frac{S_1}{R_{11}^+} \right)^2 \geq \left( \frac{S_6}{R_6} \right)^2 \quad (3)$$

– fiber-matrix shearing dominated sub-case

$$\left( \frac{S_1}{R_{11}^+} \right)^2 < \left( \frac{S_6}{R_6} \right)^2 \quad (4)$$

- Fiber – Compression ( $S_1 < 0$ )

$$f_f^- = \frac{-S_1}{R_{11}^-} \quad (5)$$

- Matrix – Tension ( $S_2 > 0$ )

$$f_m^+ = \left( \frac{S_2}{R_{22}^+} \right)^2 + \left( \frac{S_6}{R_6} \right)^2 \quad (6)$$

- Matrix – Compression ( $S_2 < 0$ )

$$f_m^- = \left( \frac{S_2}{2R_6} \right)^2 + \frac{S_2}{R_{22}^-} \left[ \left( \frac{R_{22}^-}{2R_6} \right)^2 - 1 \right] + \left( \frac{S_6}{R_6} \right)^2 \quad (7)$$

Once any of the failure modes is detected by one of the sub-criteria an appropriate degradation of selected material properties is performed in a way similar but not identical to Doh and Hong (1995). For matrix cracking transverse "matrix dominated" properties are reduced to 10 % of the original value. For fiber breakage longitudinal "fiber dominated" properties are reduced to 10 % of the initial values. Failed material properties are not set equal to zero to ensure numerical convergence, as explained below.

#### 4.3 Computational Implementation

The failure and post-failure models of Tsai and Chang have been implemented in the parameterized finite element model for composite pressure vessels as described by Krieger et al (2001). The non-linear solution is performed as an incremental succession of single load-step/single sub-step "single-frame" restart analyses in the underlying ANSYS program. After each converged load-step the failure criteria are checked on an element-by-element and ply-by-ply bases. Once a failure condition is encountered, the material properties of the concerned ply are changed by assigning a new material property set to this particular ply. Different material property sets are prepared to describe the undamaged material as well as the different damage states containing matrix cracks or broken fibers. With the modified material properties in place, the analysis is restarted for the next incremental load-step. This kind of procedure constitutes an "non-standard" application of the ANSYS program and extra care must be taken to ensure convergence of the process.

In particular, a sufficient mesh density and sufficiently small load-steps are required. If reasonable limits are observed, each load-step converges within 3 to 4 iterations. This is comparable to analyses without degradation. Under these conditions the procedure to check the failure criteria and perform the degradation takes about 50 – 75 % of the time needed to compute one converged load-step. Thus, the total analysis time with progressive degradation is also increased by about 50 – 75 %. The computational procedure has been firmly embedded in the general parameterized analysis model for composite pressure vessels and can now be used in a routine fashion.

## 6. Computational Results

The analysis program for composite pressure vessels including the described failure/post-failure models has been applied to the S33 rocket motor case (Loures et al 2001) with the aim of computing the burst pressure. This case is made of two helical layers in planar winding with an angle of  $16^\circ$  and reinforced by three hoop layers in the cylindrical part. The nominal thickness of each layer is 0.6 mm for helical layers and 0.75 mm for hoop layers. The assumed material properties for the Carbon/Epoxy material are based on the values given in Tab. (1) but were adjusted for a fiber volume fraction of 63 % using micro-mechanics.

Table 1. Material Properties (T700S/Epoxy  $V_f = 60\%$ ).

Property	Value	Test Method
Tensile Strength	2550 MPa	ASTM D-3039
Tensile Modulus	135 GPa	ASTM D-3039
Tensile Strain	1.7 %	ASTM D-3039
Compressive Strength	1470 MPa	ASTM D-695
Flexural Strength	1670 MPa	ASTM D-790
Flexural Modulus	120 GPa	ASTM D-790
ILSS	90 MPa	ASTM D-2344
$90^\circ$ Tensile Strength	69 MPa	ASTM D-3039

At this point it must be reported that, despite considerable effort, no meaningful failure/post-failure simulation and burst pressure computation using the Tsai model could be completed. This can be attributed to the inherent difficulty of distinguishing between matrix and fiber failure in this model. The artifice of using the transverse strain for this discrimination, which reportedly works in cases of laminate analyses under homogeneous loading condition, apparently fails when faced with redistributing stresses under non-homogeneous loading conditions. The reason for this is that a second failure (i.e. activation of the Tsai-Wu criterion) after a preceding matrix cracking is always interpreted as fiber breakage, leading to a premature prediction of the burst condition. In the sequel only results obtained by using the Chang model are compared with results computed without application of progressive degradation are reported.

A meridian cross-section of the motor case is shown in Fig. (3). The critical regions of aft flange, forward flange and skirt attachments are clearly visible. The computational results, namely stress-components in fiber- and transverse directions as well as displacements in shell-normal direction, will be presented along paths with coordinate  $s$  on the inside 'i' and outside 'o' surfaces. These paths are extending from the aft polar opening ( $s = -500$ ) to the forward polar opening ( $s = 550$ ). The skirt attachments are situated at  $s = -200$  and  $s = 200$ .

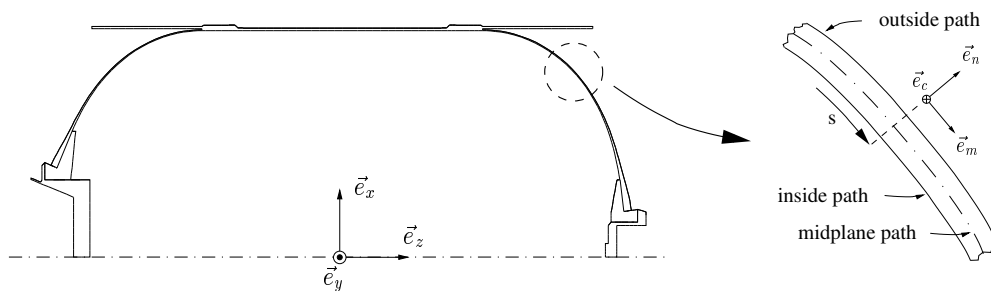


Figure 3. Meridian cross-section of the S33 motor case.

In Fig. (3) and Fig. (4) the in-plane stress-components in direction transverse to the fiber ("matrix-direction") are compared for computations with and without degradation for internal pressure of 2 MPa and 3 MPa. At 2 MPa the results are still identical but at 3 MPa the differences show the formation and distribution of matrix cracks and the resulting reduction of matrix stiffness. Because of the reduced material properties the matrix experiences less stress and carries a reduced load.

Figure (5) shows the computed stress-component in fiber direction for an internal pressure of 11 MPa. The peak stresses are increased in the degraded case owing to the reduced stiffness of the matrix. The situation after burst pressure

is show in Fig. (6): Fiber breakage is signified by high un-physical stresses in fiber direction after the material properties have been degraded to represent the loss of stiffness in the fiber direction. If the fiber-dominated material properties would have been degraded to 0, and not 10 % of the original values as in the present case, no convergence could be achieved for an internal pressure of 12 MPa. Hence, the simulation predicts a burst pressure between 11 MPa and 12 MPa. This can be compared with experimental results for different burst tests from Table (2). The predicted fiber breakage, and hence the burst pressure, depends critically on the shear-stress interaction in the fiber-breakage sub-criterion in Eq. (2) since the stress value for  $\sigma_{11}$  of about 2000 MPa is still well below the assumed uniaxial composite tensile strength.

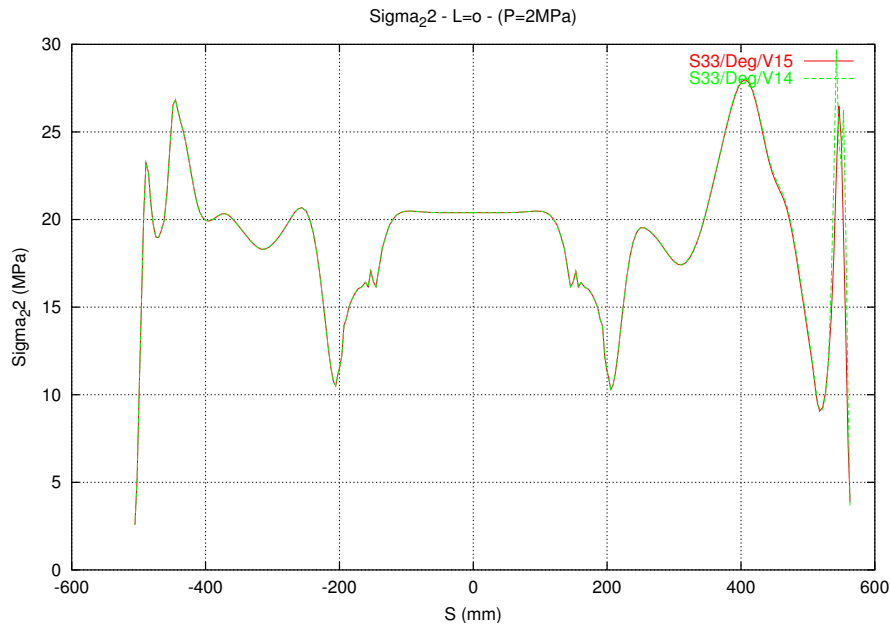


Figure 4. Transverse Stress  $\sigma_{22}$  at 2 MPa internal pressure. Simulations with (V14) and without (V15) progressive degradations give still the same results as no failure has occurred.

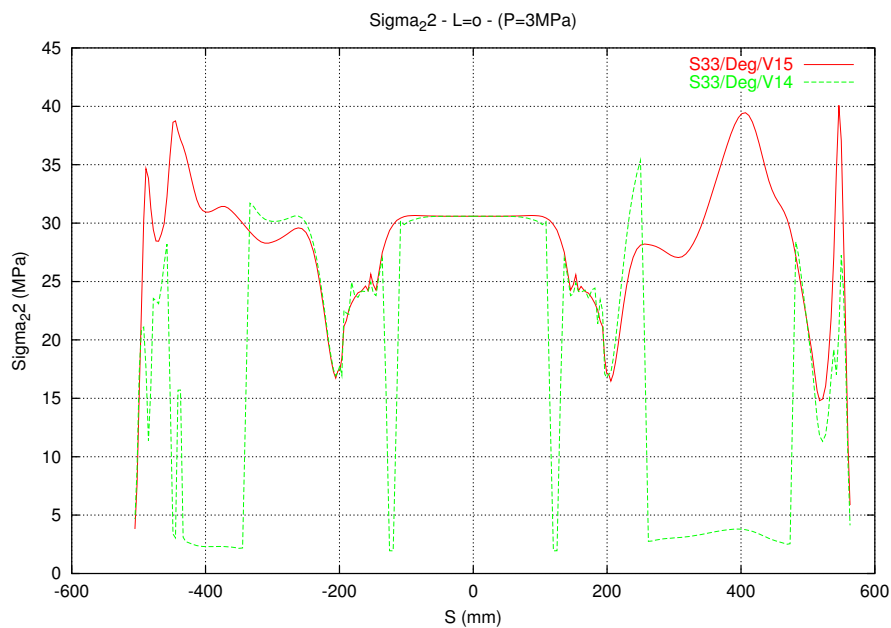


Figure 5. Transverse Stress  $\sigma_{22}$  at 3 MPa internal pressure. The simulation with progressive degradation (V14) shows matrix cracking by reduced transverse stresses. This effect spreads throughout the entire structure as the load is further increased.

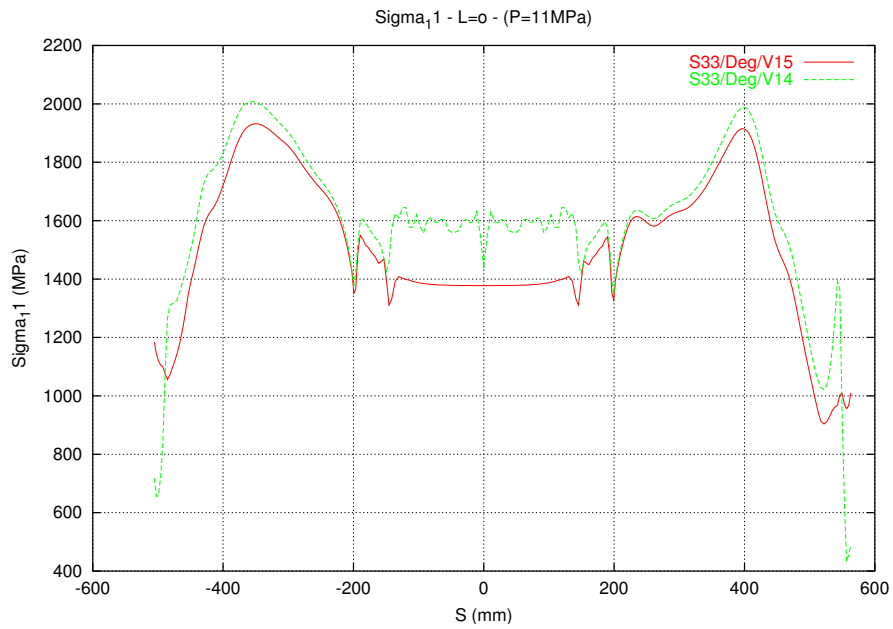


Figure 6. Longitudinal Stress  $\sigma_{11}$  at 11 MPa internal pressure. The simulation with progressive degradation (V14) predicts about 5 % increased peak stresses in the critical regions since the stiffness of the matrix has been reduced.

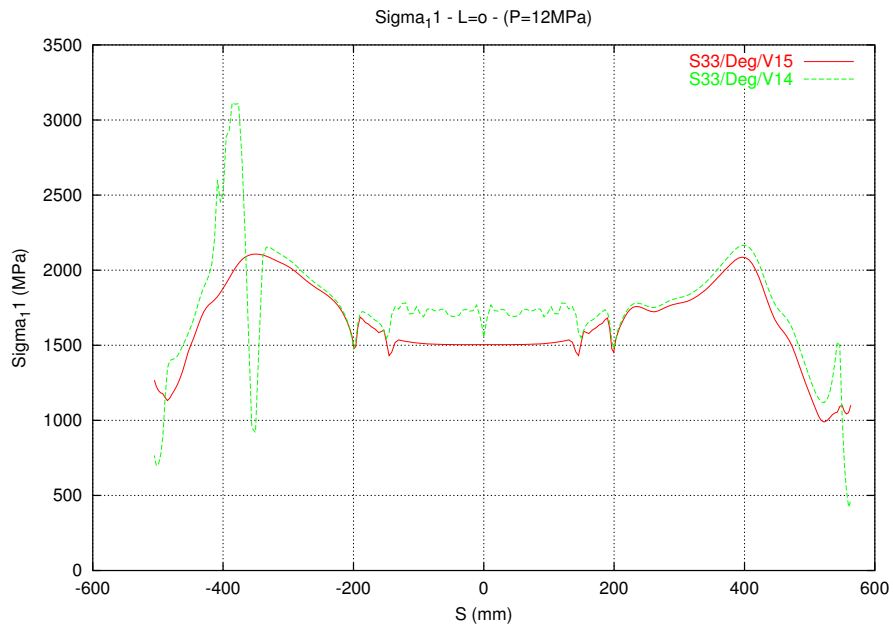


Figure 7. Longitudinal Stress  $\sigma_{11}$  at 12 MPa internal pressure. The burst condition is signified by un-physical high stresses in the area of fiber breakage (aft dome) after material properties have been degraded. (The solution is converged but *does not* represent a physically attainable state of the structure.)

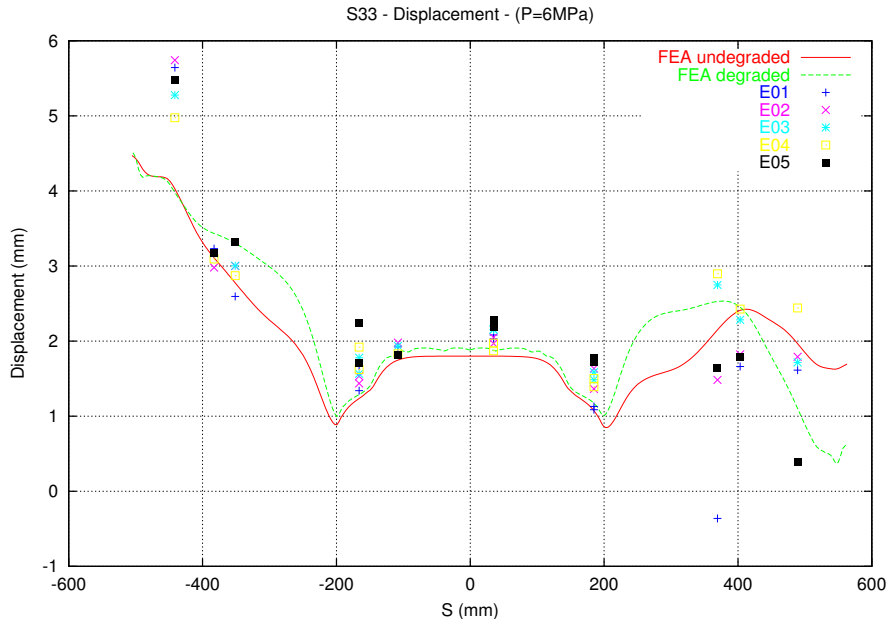


Figure 8. Displacement in Normal Direction  $u_n$  at 6 MPa internal Pressure.

Displacements in shell-normal direction, computed for an internal pressure of 6 MPa (operating pressure) with and without degradation, are compared with measurements from different pressure vessel specimens in Fig. (7). The computed deformations are quite distinct if degradation is taken into account, but scatter of experimental data and lack of measurements in the most interesting locations makes a final assessment difficult.

Table 2. Experimental Burst Pressure for different S33 rocket motor cases.

Test	1	2	3	4	5
Burst Pressure (MPa)	8.65	11.2	12.1	10.5	11.28

## 7. Conclusions

Full-scale high-resolution models of composite solid rocket motor cases are build using existing layered volume elements. Axisymmetric coupling conditions are used to enforce an axisymmetric solution without artificial stress perturbations. One element in circumferential direction is sufficient, which reduces the computational effort and makes these models affordable for use on personal computers even for nonlinear analyses. Two different failure/post-failure models are implemented in the overall pressure vessel simulation and enable a progressive degradation analysis up to burst-pressure. The model proposed by Tsai was found to be ineffective in the present situation and may need additional modifications for a successful application. The model proposed by Chang enables an effective distinction between the two important failure modes of matrix cracking and fiber breakage. The predicted value for the burst pressure is in good agreement with the experimental results but depends critically on the shear-stress influence in the fiber-breakage sub-criterion. This deserves further consideration. The location of the fiber breakage, leading immediately to the burst condition, is predicted in the same region as observed in the experiments. Comparison of computed and measured deformations is inconclusive, since measurements are lacking in the most interesting regions. It is remarkable that the process of matrix cracking is apparently already finished when the operating pressure is reached and leads to a significantly different deformation behavior. The internal pressure can be almost doubled before failure of the vessel occurs.

The progressive degradation analysis gives detailed information about the mechanical behavior of the structure, improves the understanding of the failure process and can be used for optimizations and also for analysis and design of future pressure vessels.

## 8. Acknowledgment

This work was supported by a research grant of the German National Science Foundation (DFG) under project number Be 766/40-2. The bilateral cooperation between IAE and MMW is supported by the International Bureau of the German Ministry for Education and Research (BMBF) at the German Aerospace Center (DLR) under project number BRA 99/02. This support is gratefully acknowledged.

## 9. References

- Chang, F.K. and Chang, K.Y., 1987, "A Progressive Damage Model for Laminated Composites Containing Stress Concentrations", *Journal of Composite Materials*, Vol. 21, pp. 834-855
- Doh, Y.D. and Hong, C.S., 1995, "Progressive Failure Analysis for Filament Wound Pressure Vessel", *J. of Reinforced Plastics and Composites*, Vol. 14, pp. 1278-1306
- Gramoll, K.C., Namiki, F. and Onoda, J., 1990, "General Structural Analysis of an Upper Stage Composite Rocket Motor Case", *Proceedings of the 17th International Symposium of Space Technology and Science*, Tokyo, Japan
- Hashin, Z., 1980, "Failure Criteria for Unidirectional Fiber Composites", *Journal of Applied Mechanics*, Vol. 47, pp. 329-334
- Isakowitz, S.J., Hopkins, J.P. and Hopkins J.B., 1999, "International Reference Guide To Space Launch Systems", AIAA, pp. 487-500
- Jones, R.M., 1999, "Mechanics of Composite Materials", 2nd ed., Taylor & Francis, Philadelphia
- Krieger, J., Multhoff, J.B., Loures da Costa, L.E.V. and Betten, J., 2001, "Development of a Finite Element Model for Composite Pressure Vessels and its Application in Structural Optimization", *Proceedings of COBEM 2001, Aerospace Engineering*, Vol. 6, pp. 366-375
- Liu, K.-S. and Tsai, S.W. "A Progressive Quadratic Failure Criterion for a Laminate", 1998, *Composite Science and Technology*, 58, pp. 1023-1032
- Loures da Costa, L.E.V., Multhoff, J.B., Krieger, J. and Betten, J., 2001, "Structural Development of the S33 Rocket Motor Case", *Proceedings of COBEM 2001, Aerospace Engineering*, Vol. 6, pp. 237-246
- Nahas, M.N., 1986, "Survey of Failure and Post-Failure Theories of Laminated Fiber-Reinforced Composites", *Journal of Composite Technology & Research*, Vol. 8, No. 4, pp. 138-153
- Multhoff, J.B., Krieger, J., Loures da Costa, L.E.V., and Betten, J., 2001, "Problems in High-Resolution Finite Element Models of Composite Rocket Motor Cases", *Proceedings of COBEM 2001, Aerospace Engineering*, Vol. 6, pp. 207-216
- Ochoa, O.O. and Reddy J.N., 1992, "Finite Element Analysis of Composite Laminates", Kluwer Academic Publishers, Dordrecht
- Ore, E., 1998, "Nonlinear Stress Analysis at Burst Condition of Composite Pressure Vessel", *Proceedings of the ANSYS Conference*, Pittsburgh, USA
- Pereira, J.C. and Palmerio, A., 1998, "Failure Analysis of a Filament-Wound Pressure Vessel", *Proceedings of the ANSYS Conference*, Pittsburgh, USA
- Policelli, F.J. and Vicario, A.A., 1987, "Space and Missile Systems", *Engineering Materials Handbook, Composites*, Ed. T.J. Reinhard, 3rd ed., ASM International
- Rosato, D.V. and Grove, C.S., 1964, "Filament Winding: Its development, manufacture, application, and design", John Wiley & Sons, New York
- Shu, J.C., Chiu, S.T. and Chang, J.B., 1995, "An Enhanced Analysis Method for Composite Overwrapped Pressure Vessels", AIAA, *Proceedings of the 36th Structures, Structural Dynamics and Materials Conference*, New Orleans, pp. 394-403
- Sutton, G.P., 1992, "Rocket Propulsion Elements: An Introduction to the Engineering of Rockets", 6th ed., John Wiley & Sons, New York
- Sun, X.-K., Du, S.-Y. and Wang, G.-D., 1999, "Bursting problem of filament wound composite pressure vessels", *Int. J. of Pressure Vessels and Piping*, Vol. 76, pp. 55-59
- Tsai, S.W. and Wu, E.M., 1971, "A General Theory of Strength for Anisotropic Materials", *Journal of Composite Materials*, Vol. 5, pp. 58-80
- Tsai, S.W., 1992, "Theory of Composite Design", Think Composites, Dayton, Paris, Tokyo
- Wood, J., 1994, "Finite Element Analysis of Composite Structures", *Composite Structures*, Vol. 29, pp. 219-230

## 10. Copyright Notice

The authors are the only responsible for the printed material included in this paper.